The Role of Catastrophic Floods Generated by Collapse of Natural Dams Since the Neolithic in the Oases of Bukhara and Qaraqöl: Preliminary Results

Eric Fouache, Rocco Rante, Djamal Mirzaakhmedov, Rachid Ragala, Malvina Dupays, Claude Vella, Jules Fleury, Valérie Andrieu-Ponel, Antoine Zink, Elisa Porto, et al.

International Journal of
Geohazards and Environment
http://ijge.camdemia.ca, ijge@camdemia.ca
IJGE 2016 **2**(**3**): 150-165
Available at http://ojs.library.dal.ca/ijge

Technical Notes

The Role of Catastrophic Floods Generated by Collapse of Natural Dams Since the Neolithic in the Oases of Bukhara and Qaraqöl: Preliminary Results

Eric Fouache[1*], Rocco Rante[2], Djamal Mirzaakhmedov[3], Rachid Ragala[4], Malvina Dupays[5], Claude Vella[5], Jules Fleury[5], Valerie Andrieu-Ponnel[6], Antoine Zink[7], Elisa Porto[7], Frédérique Brunet[8], Lucie Cez[8]

[1]University Paris Sorbonne Abu Dhabi, UMR 8185 ENEC, UAE/France
[2]Louvre Museum, Paris and ArScan, UMR 7041, France
[3]Archaeological Institute of Samarkand, Ouzbekistan
[4]University Paris Sorbonne Abu Dhabi, UMR 8557, CAMS-CNRS-EHESS, UAE/France
[5]Aix Marseille Université AMU-CNRS, CEREGE UMR 7330, France
[6]Aix Marseille Université, IMBE CNRS, IRD, Avignon Université, Europôle Méditerranéen de l'Arbois, BP 80, 13 545 Aix-en-Provence Cedex 4, France
[7]Centre de restauration et de recherche des musées de France, Ministère de la Culture et de la Communication, France
[8]CNRS, ArScan UMR 7041, France

Abstract: The history of the civilizations of the oases of Bukhara and Qaraqöl (south-eastern Uzbekistan) since the Neolithic in relation to environmental changes is studied by the French/Uzbekistan Archaeological Mission in Bukhara[1] following pioneering Russian studies[2]. Using a methodology tested in Afghanistan, the geoarchaeological side of the program focused on the drawing of a regional geomorphological map then on the identification, mapping and dating of the paleochannels of the river Zerafshan. We established the chronology of several generations of fluvial channels in relation to archaeological settlements of different eras (Early Neolithic, Neolithic, Bronze Age, Iron Age and Islamic period) and with optically stimulated luminescence dating of alluvial deposits. Based on preliminary results of these OSL dates we propose and discuss a regional environmental reconstruction. We hypothesize that the main cause of avulsion could be catastrophic floods generated by collapse of natural dams in the upper part of the Zerafshan River.

Keywords: geoarchaeology, fluvial geomorphology, geohazard, OSL dating, tributary migration, Uzbekistan

1 Introduction

In 2009, the Department of Islamic Art of the Louvre Museum, in collaboration with the French Ministry of Foreign Affairs and the Archaeological Institute of Samarkand and the Uzbek Academy of Sciences, opened an archaeological mission in the Bukhara oasis and started a program of surveys and excavations over the whole oasis, recording more than 1173 archaeological sites, from the Neolithic to present times, including the extension of Qaraqöl area, as far as the Amu Daria (Oxus) (Fig. 1). Today the river Zerafshan flows in a North-East/South-West main channel to which a dense network of irrigation and drainage channels is connected. Looking at a regional map or a satellite image (Fig. 1), it is obvious that many of these channels

* Corresponding Author: Eric Fouache, Email, eric.fouache@psuad.ac.ae, Tel: +97 (150) 2632-323

DOI: 10.15273/ijge.2016.03.015

follow paleochannels of the river Zerafshan and that this river underwent important changes over the Holocene.

Using a methodology tested in Afghanistan (Fouache et al 2012), we surveyed the geological, tectonic, geomorphological, climatological and hydrological aspects of this area. This facilitated our reconstitution of the channels occupied by the Zerafshan River since the Last Glacial Maximum, and samples for OSL dating were retrieved from five different paleochannels. Taking into account the importance of geomorphological dynamics is a necessary prerequisite for reconstructing the location and chronology of irrigated soils at different times. A similar research strategy was adopted around the site of Aï Khanum upstream from the plain of Balkh on the left bank of the Amu Daria (Gardin and Gentelle 1979) or for the Balk River, also in Afghanistan. Our study demonstrates the extreme mobility of the channels of the Zerafshan River, also known as Polytimetus River by ancient Greek geographers or as Sught River by the Persians, and the scope of those shifts over a distance of 100 km over the past 10,000 years. Those shifts caused a displacement of human settlements and main roads.

Figure 1. Study area - World Imagery ArcGIS ESRI. Color composite – Blue, Green, Red. The image was our main source for the drawing of the geomorphological map

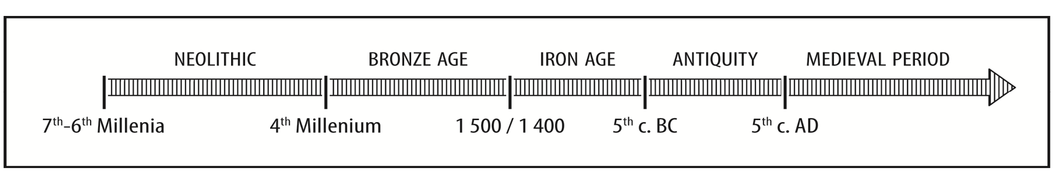

Figure 2. Historical table

1.1 Historical Context

Archaeological evidences of the Neolithic occupation around the Bukhara oasis have been brought to light by recent researches. For fifteen years, the archaeological missions, first Uzbeko-Polish, then Uzbeko-French (Brunet 2005), have focused their efforts on the site of Ajakagytma, in the northern part of the Bukhara oasis, with the aim to better understand the Kel'teminar culture. Artefacts belonging to this culture, which thanks to this recent research could be globally dated to the 7th - 6th and 4th - 3rd millennia, could be also found south of the Bukhara oasis, around the Kum Sultan area, as well as along the ancient path of the Kashka Daria[1].

Neolithic, but especially Bronze Age traces have been brought to light by Guljamov, in the mid-20th century, in the Zamanbaba region, southwest of the oasis (Askarov 1965, Guljamov et al 1966, Askarov 1981).

The period between the Late Bronze Age and the Early Iron Age is less well known. The mid-first millennium BCE seems to be characterized by occupation in the western part of the Bukhara oasis, west of Varakhša[2] (Bash tepe, Urta tepe, Ayak tepe and others), in which different surveys showed the presence of distinctive cultural markers of this epoch, such as cylindrical and cylindro-conical vases (Adylov 2002).

Some scholars recognise pottery influences from the 4th and the 2nd century BCE coming from Afrasyab and Khorezm (Lo Muzio 2009). By the 4th century BCE, Central Asia was characterized by the Grek occupation and later by the birth of the Greek-Bactrian Kingdom. The Bukhara oasis was not spared this massive cultural occupation, also identifiable in Bactriana, as well as in Samarkand. Greek cultural influences have been discovered also within the Bukhara oasis, such influences coming from the eastern and southeastern regions.

Later, by the 2nd - 1st centuries BCE, the oasis was occupied by populations coming mostly from the north and the northeast, called K'ang-chü (Litvinskij 1972 and 1976) in the Chinese sources, which settled within the oasis. The regions to the west of the oasis, behind the Varakhša area, as well as that southwest around Zamanbaba, were gradually depopulated by at least the end of the Bronze Age, even if the latest research in this zone directed by Sören Stark (University of New York-Archaeological Samarkand Institute) brought to light evidence of some 5th century CE occupations[3], showing the presence of water supply probably coming in seasonal groundwater flows.

By the mid-4th century CE the oasis experienced several other migrations of nomad confederations, which were most probably located in the middle Sir Daria. This cultural phase presents several markers, which are clearly identifiable, especially on pottery (Burjakov and Košelenko 1985)[4].

The 6th - early 8th centuries are characterized by the occupation of Turkish populations, the last ruling elite before the Islamic conquest, which took place at the beginning of the 8th century.

By the 9th century, Islamic occupation took place mostly within the inherited cities. Sometimes rulers founded new unwalled cities close to the previous fortified ones. At that epoch, the oasis was already highly urbanized, made possible by the intensive organisation and reorganisation of water irrigation channels.

Irrigation of the floodplains, possible because the Zerafshan River is a perennial one, was indispensable for agriculture and to sustain the development of the Bukhara oasis, as well as Qaraqöl oasis, throughout its history. A complete understanding of the historical and archaeological evolution in this area requires the reconstruction of the Zerafshan river course, how it modified the floodplain and how this showed in the development of the oasis of Bukhara.

---

[1] Some of these artefacts have been characterized thanks to Frédérique Brunet (CNRS, UMR 7041), director of the Franco-Uzbek mission MAFANAC-Ajakagytma.

[2] Even if in a later period, Šiškin (1955 and 1963) published the results of a large survey carried out in this area as well as the excavation of Varakhša.

[3] See also Rante 2013.

[4] Data gave during a study days (October 7 - 9, 2015) organised at the University of Hamburg by Stefan Heidemann.

1.2 The geological and tectonic setting

The joint oases of Bukhara and Qaraqöl are located in central Uzbekistan. Covering approximately 1333 km^2, they are bounded to the north by the Kysyl Kum desert, a huge erg, and to the south by the Kara Kum desert. To the west flows the Amu Darya river with a South/North course. To the East the Zerafshan valley is limited by Cretaceous limestone ranges.

This area (Bossu 1996) is affected by the Himalayan collision (Fig. 3). Active South-East/North-West slip faults can be observed as well as overlapping fronts in a context of compression as can be seen along the Kouldouktou chain, north of the Bukhara oasis. Between the oases of Qaraqöl and Bukhara there is a Neogene horst plateau composed of clay, gypsum, limestone and conglomerates. Our study area is composed of alluvial plains, with an average altitude of 260 m to the East and 200 m to the West on a 200 km long transect, that have been actively subsiding area during the Plio-Quaternary period. Active tectonics is attested by the 818 AD earthquake in Gazli, which underwent another one of a magnitude of 7 on the Richter scale in 1984.

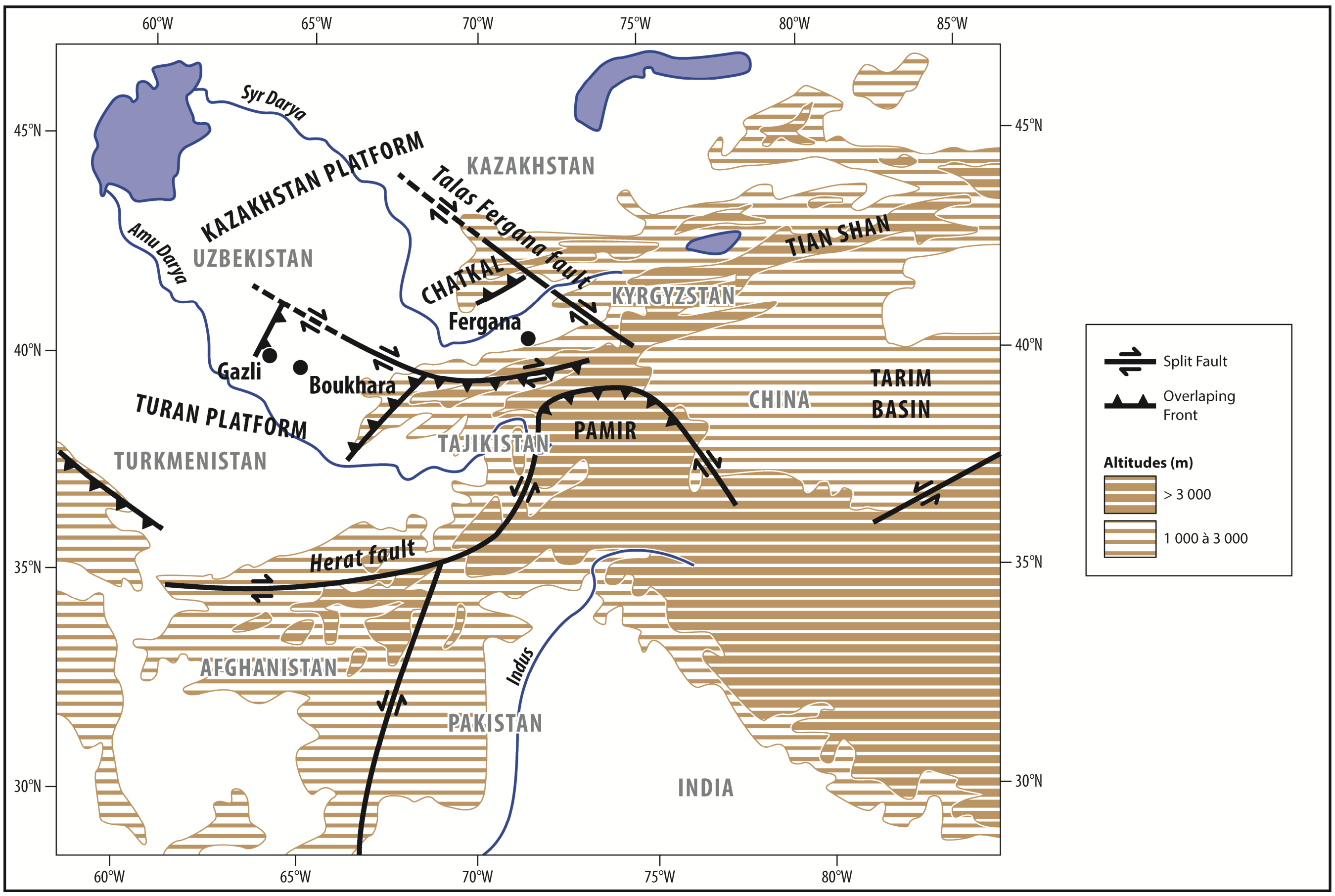

Figure 3. Tectonic map of the broader study area

1.3 Hydroclimatic data

During the last glacial period, the Zerafshan river had a regime of spring and summer time discharges that were torrential and built a vast alluvial plain. Since the lateglacial period, the river has become an endorheic perennial river with permanent discharge.

The climate of Bukhara oasis is arid cold desert. The water from the Zerafshan river is the only source of water for agriculture and human activities. The Zerafshan river, with a drainage basin of 143,000 km^2, originates 741 upstream from the Alai Mountains and the Zerafshan glacier in Tadjikistan. It has a nivo-glacial hydrological regime and 97% of its discharge is generated in Tadjikistan. At the Ravatkhodja dam station just on the border between Tadjikistan and Uzbekistan, the mean annual discharge is 170 m^3/s. Until the 1960s, Bukhara oasis received water for irrigation only from the Zerafshan river. In the beginning of the 1970s, a canal from Amu Daria to the oasis of Bukhara was built. Today some 1.2 million people live in Bukhara oasis and more than 230,000 ha of land are irrigated. In the end of the 1980s, Bukhara oasis started to face serious water-environmental problems such as land salinity water-logging (Abdullaev 2004) and anthropogenic pollution (Olsson et al 2013). Seasonal flooding was beneficial and never seen as a hazard.

2 Methodology

Geomorphological mapping of paleo-channels within the Bukhara and Qaraqöl plains relied on 1/50,000 Russian topographical maps and on spatial imagery (Landsat ETM+ 13-04-2006) drawn with ArcGIS and Idrisi Selva software. The creation of databases for the Zerafshan river and its paleo-channels is based on a methodology using a multi-source Geodatabase. All the data are georeferenced in the same geographic reference (GCS-WGS1984).

The middle infrared image of Landsat ETM + was of great help. Indeed channel 7 (MIR) brings out rivers, water surfaces and humid areas. Also the application of Laplacian filter (3 × 3) to the same channel has allowed edge enhancement and therefore the detection of linear forms. This method (Fig. 4) facilitated the identification and digitization of paleo-channels.

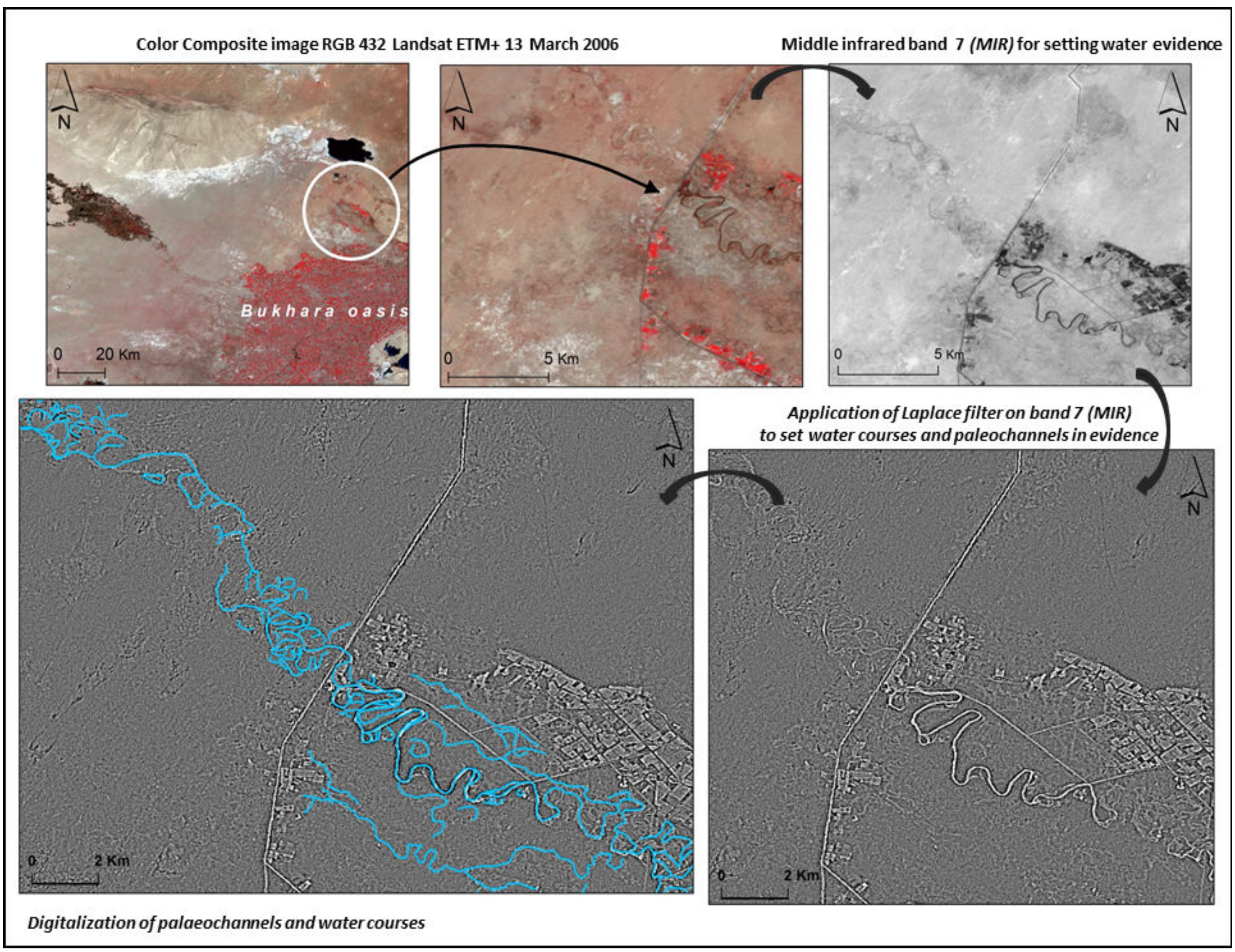

Figure 4. Methodological steps in remote sensing data analysis to determine and visualize the paleo-channels, combining middle infrared band and Laplace filter

The map generated by remote sensing data was tested and verified by geomorphological mapping and field observations, which had resulted in identifying 8 generations of paleo-channels that we attempted to date by relative and absolute dating methods. We argue that the location of the settlements with regard to the channels allows relative dating of some generations, essentially from the Neolithic to the Bronze Age period. In order to establish an absolute date, we used OSL on samples taken down to 2 m depth from different salty sand sedimentary layers from 5 paleo-channels identified on image and in the field. These two chronological approaches (archaeological mapping and OSL dating) allowed us to reconstruct the generations of paleo-channels and to shed some light on the geomorphological evolution of the Bukhara and Qaraqöl plains since the end of the Upper Pleistocene. Based on the good results obtained by this OSL method, we decided to complete the sampling during spring 2016 on the last 3 paleo-channels that have been identified.

2.1 Granulometric analyses

Various sedimentological analyses have been carried out: texture analysis, % organic matter, % CaCO3, mechanical and laser granulometry and grain morphoscopy.

Particle size analyses were carried out on well sediments. The samples were mingled with a dispersing agent (0.5% sodium hexametaphosphate) dissolved in distilled water and shaken for 2 hours in order to disperse clay aggregates. Ultrasonic dispersion on the sediment was maintained during the laser diffraction measurement. The particle size distribution was measured with a laser granulometer (Coulter LS 230), in an interval of 0.04 to 2000 microns. The calculation model (software version 2.05) used the Mie theory and the Fraunhofer approximation.

2.2 Luminescence dating

Eight sedimentary beds of 10 to 100 cm, on five paleo-channels, were sampled (Fig. 5) for luminescence dating with metallic tubes (20 cm long by 5 cm diameter) and described. The Munsell colour scale was used to describe the colours. They were later opened in the laboratory under dim red lighting. Grains were sampled from the inner end of the tubes. The first 2 cm were removed to avoid contamination. The sediment was moistened locally to avoid mixing grains from different depths. A sample was obtained by pressing a 1 cm diameter plastic tube inside 4 cm. The external 2 cm of the sample were used for evaluation of the content in radionuclides.

Figure 5. Photograph of one OSL sampling in Bash Tepe Trench (OSL 1 & 2; Location and detail in Figs. 6 and 7)

The other 2 cm were etched by hydrogen peroxide (9%wt, to eliminate the organic materials) and by hydrochloric acid (10%, to eliminate carbonates). The sand-sized (50 - 80 µm) polymineral fraction was selected by dry sieving and deposited using a 4 mg spoon on aluminium cups. Four discs for each sample were prepared for Optically Stimulated Luminescence (OSL) dating.

Equivalent dose determination

The luminescence measurements were performed with a Risø TL/OSL DA-15 set fitted with a 90Sr/90Y source delivering 6.87 Gy/min on Jan 1,2008, and all measurements were made using an EMI 9235QA photomultiplier. The luminescence was detected through a 7.5 mm thick U-340 filter. To prevent unwanted exposure and stimulation of adjacent aliquots, the discs were placed only on the odd positions.

The equivalent doses were obtained by applying a double single aliquot regenerated OSL (OSL-SAR) protocol with the use of infrared stimulation (IR laser diode 830±10 nm; 50% of 450 mW/cm^2 full power at 60°C for 100 s) prior to blue stimulation (21 blue diodes pairs 470±30 nm; 50% of 19 mW/cm^2 full power at 125°C for 100 seconds). For each sample we used four aliquots corresponding to four different temperatures: 250°C, 275°C, 300°C and 325°C (Zink et al 2013). Fading rates were measured using a SAR fading protocol (Zink 2008).

Dose rate determination

In situ gamma spectrometry measurements were performed in Tarab trench on May 3, 2014, with a NanoSpec (Target Systemelectronic gmbh) portable multichannel analyser using a 2" × 2" NaI (Tl) probe. The probe was introduced 30 cm deep inside the sediment. The calculation of the dose rate was done using a threshold technique on the entire spectrum between 500 keV and 2780 keV. The radionuclides contribution was based on the windows technique (Aitken 1985).

Laboratory measurements were made on the external part of the sampling tubes. Internal uranium and thorium content was estimated using alpha counting conducted in a Daybreak 582/583 alpha counter. The uncertainty of the radionuclide was taken equal to 10% corresponding to sediment inhomogeneity. It is larger than the measurement uncertainty. The first attempt to measure the potassium content in laboratory using scanning electronic microscopy coupled with energy dispersive spectrum (SEM-EDS) failed due to the high carbonate content. The uranium and thorium contents measured in laboratory for Tarab samples fit well with the values estimated from the *in situ* gamma spectrometry. As the uranium and thorium contents are similar for the different sites, we assume a good homogeneity for the potassium content too, and use potassium contents measured in the Tarab trench for the whole site. Using Zimmerman's attenuation factors (1971), we opted for a cautious 5.0±3.0% water content.

Cosmic ray contribution was calculated for each sample. For convenience, the correction of cosmic dose rate due to depth into the soil (Prescott and Hutton 1994) was based on the present depth.

3 Results

3.1 Geomorphological analysis

The study area comprises a series of coalescing, successive alluvial fans built up by the Zerafshan river since the end of the last Ice Age. Within this environment, the geomorphological analysis enables to identify fossil and active river forms and to reconstruct a relative timeline tying together the establishment of the fans and their associated channels. Preliminary interpretation employed a colour composite ETM` Landsat image (Figs. 1 and 4) and apart from the present channels of the Zerafshan river, a dense network of irrigation canals can be identified both on the ETM` Landsat image and 1/50,000 1989 topographic map. The most important canals utilise the flow directions of former riverbeds that were abandoned during the successive avulsions.

The present day main channel of the Zerafshan river is oriented North-East/South-West, but we were able to map 8 different generations of paleo-channels oriented East/West (Fig. 6).

The plateau between Qaraqöl plain and Bukhara plain is cut by an active narrow valley today and a paleo-one 5 km on the west. Throughout the Holocene, there was a progressive shift of the active fan's apex by about 80 km south westwards.

The stratigraphy of the sediment from the downstream course of the river Zerafshan has been described on trenches or on gravel pit front faces (Fig. 7). We will only present the main results which allow to help interpret the morphology observed in the field and by imagery.

3.2 Stratigraphy and sedimentology descriptions

Five different areas were studied, each corresponding to a paleo-channel of the Zerafshan river. The site which is furthest to the East (Fig. 7: North/East trench, OSL7) is located upstream from a river bifurcation of the Zerafshan in the upper part of the alluvial fan formed by the Zerafshan in the Kyzyl Kum desert. The deposit observed on the forehead of the cut of a gravel pit is composed of two overlying alluvial sequences. At the bottom of the first sequence we find a thick layer (more than 60 cm) of multi-centimetre pebbles making up more than 83% of the sediment in a sandy matrix. The bottom layer is topped by a 15 cm thick layer of fine sand (11%). This overall fine layer (the average grain-size is 115 microns, the main mode 140 microns) is relatively poor in organic matter (1%) and marked by an enrichment in fine particles (Sk = 0.47). The whole sequence shows a subparallel, subhorizontal stratification. The second sequence is formed by another layer of pebbles and granules for 93% but smaller than in the bottom layer. The gravels and granules are wrapped in a rare sand matrix (7%). Globally decreasing in grain-size, the 30 cm thick layer gradually shifts from brown-coloured, fine sand

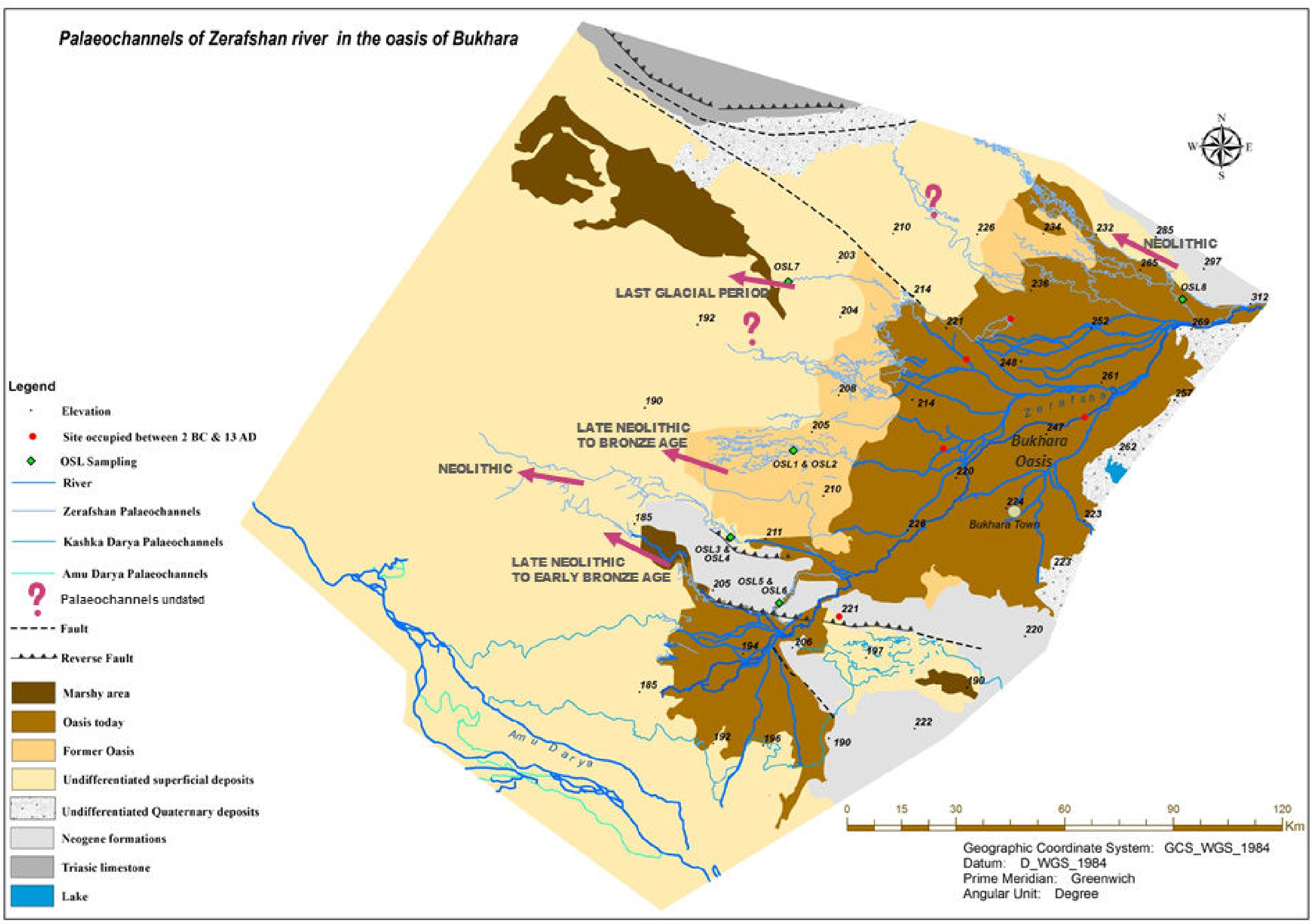

Figure 6. Geomorphological map interpreting and classifying the paleo-channels of Zerafshan river in the Bukhara and Qaraqöl oasis, in combination with the OSL sample positions, the archaeological sites and the geological structures of the study area

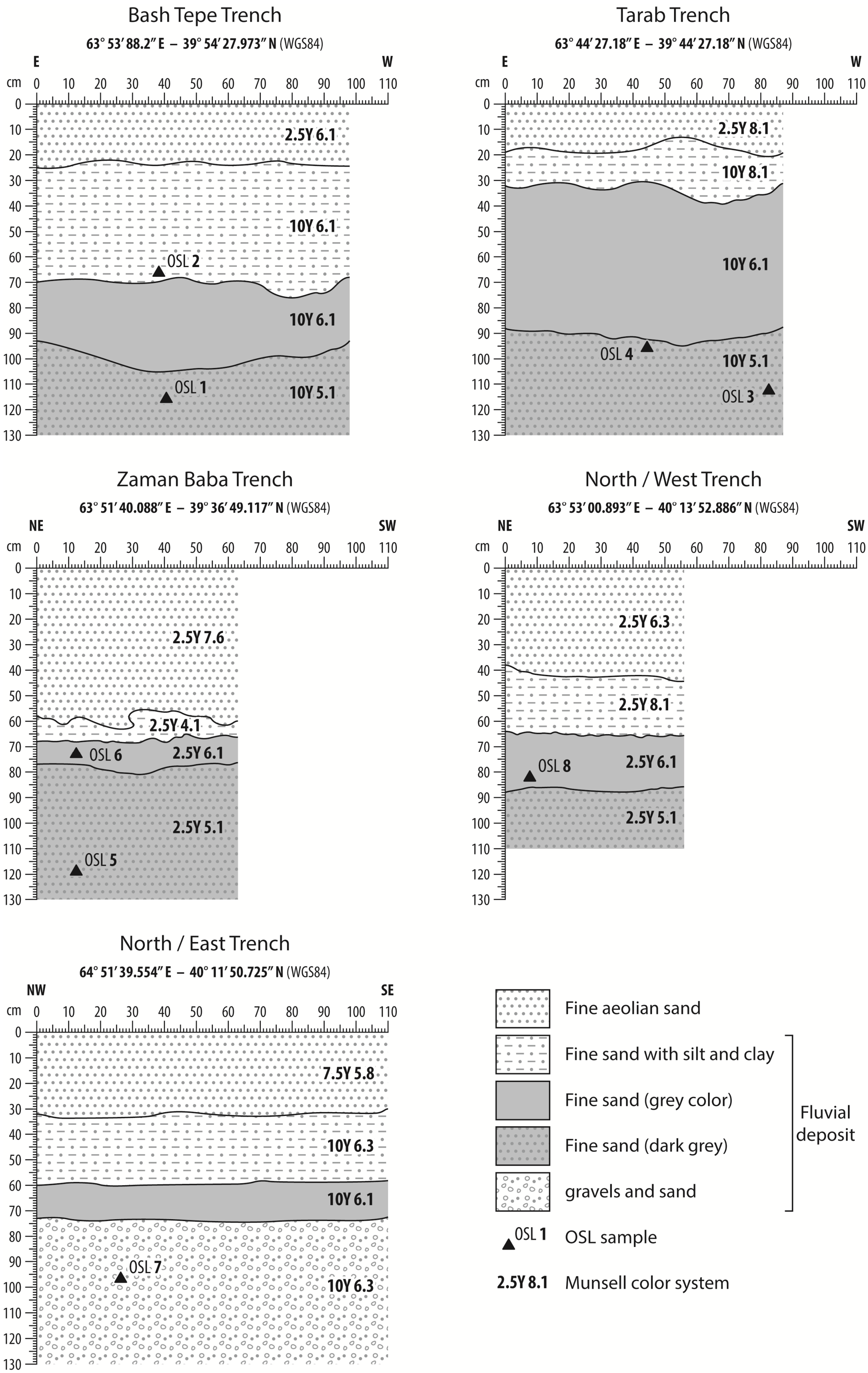

Figure 7. Stratigraphy and OSL sample locations in five trenches described to the text

(82%) to very rare gravel. The top layer is approximately as thick as the previous one (30 cm).

The second study zone is located completely downstream from another bifurcation of the Zerafshan. This branch, which is close to Vabkent and Zandana tepe (Fig. 7: North/West trench, OSL8), bifurcates 25 km downstream from the previous bifurcation. The stratigraphic observations carried out on manual drills were done at the downstream end of this branch. The stratigraphy is composed of 4 layers of fine silt and sand, the first three showing internal structures with subparallel, subhorizontal stratification. The last, massive one with a few granules also differs with its brown colour.

The third stratigraphical sequence (Fig. 7: Bash Tepe trench, OSL1 & 2) was studied on the branch close to Romitan and Bash tepe, also located downstream along the river. At the bottom, a layer of fine sand and rare granules was deposited in successive subparallel, subhorizontal beds. A layer of fine sand tops the previous one with the internal micro-bedding system. Two layers of fine massive sand top the preceding deposits. The branch of the Tarab (Fig. 7: Tarab trench, OSL4) is located further West and from a bifurcation of the Zerafshan which is further downstream than the previous ones. The stratigraphy of the previous one is situated in the final part of the bifurcation, thus, in similar hydrodynamic environments.

Beyond the stratigraphic observations made on manual drills, sedimentological analyses were carried out on three of the four layers observed. At the bottom, a layer of fine bedded sand characterized by an average grain-size of 76 microns, a proportion of organic matter of 1.5% and 17% of $CaCo_3$ and an asymmetry in the small sizes. The sand layer seems to indicate a weak energy environment.

The layer topping the previous deposit is about 60 cm thick, formed by a majority of fine bedded sand but with an average grain-size of 160 microns. The following layer is even finer, silty-clayey, and seems to form the end of the alluvial sequence. Indeed, the proportion of sand and fine earth is about 50% each. The massive yellowish sand at the top looks totally different from the underlying layers.

The last of the studied branches, furthest west, is the one heading toward Zamanbaba (Zamanbaba trench). The trench was dug upstream from the branch. The stratigraphy is very close to the previous one. It is composed of four layers, the first three of which seem to constitute a homogenous sequence decreasing in grain-size. The first layer is formed by a majority of fine sand (63%) and average-sized sand (30%), the fine sand largely dominates in the second layer (87%) while the third layer is composed mostly of fine sand (66%) and silt (24%).

The top and the bottom of the layer are very irregular in their contact with the surrounding layers and there are inclusions in the upper layer. The layer that closes the stratigraphy is very similar to the top layer of the Tarab branch by its colour and grain-size. The mainly sandy texture includes the largest proportion of average-sized sand (40%). The structure is massive and the granulometric analysis shows well-sorted sediment with a marked mode around 270 microns and a slight asymmetry towards the fine sediment. The quartz grains observed on this layer with a binocular magnifying glass are mat and almost blunt.

3.3 Interpretation

The stratigraphy observed in the section face is typical of alluvial deposits and composed of two sequences with decreasing grain-size. The base of the sequences is made up with the bottom load deposit of alluvial channels that are sufficiently dynamic to carry small pebbles and very numerous gravel and granules. The first sequence ends on a fine deposit characteristic of a river bank or a floodplain. The shape of the unimodal, rather leptokurtic granulometric curve indicates a rather good sorting of the sediment despite an enrichment in fine material which could be linked to overflow. The return to active fluvial dynamics in the second sequence may be interpreted either as a form of alluvial mobility or as a hydrological variation of this branch.

The stratigraphy observed in the Zaman Baba trench (Fig. 7 OSL5 & 6) is composed of much finer sediment than the previous one because of its location at the far end of the stream. It is composed of a sequence decreasing in grain-size interpreted as a fluvial deposit topped by aeolian deposits. For lack of further sedimentological analyses, this interpretation is grounded on a comparison with the stratigraphies and the analyses carried out on the other branches.

The stratigraphy close to Bash tepe is interpreted as an alluvial sequence with a weak carrying capacity where the two bottom layers of fine bedded sand make up an alluvial sequence of weak intensity. The two top massive layers with disorganised grains may have been put in place by the wind.

Because of their fineness and the presence of micro-laminae in the bottom layers, the deposits of the Tarab branch seem to be very similar to those observed on the Vabkent and Bash tepe branches. The laminations seem to indicate a better sorting in the bottom layers, which could be associated with a weak-energy flow. The energy of the bottom alluvial sequence seems to be decreasing owing to the increase in the proportion of fine material at the top of the sequence. The top deposits are completely different by their colour and the lack of bedding.

The sedimentary sequence of Zaman Baba made up of the first three layers is considered as a channel silting alluvial deposit with a very weak dynamic intensity. The sandy then silty character of the layers is a sign of the decreasing intensity of the flows. The contact limits of the more silty top layer is probably warped by rather important thixotropic phenomena, even leading to an injection of material in the top sandy layer, unless it is a form of aeolian erosion. The thixotropy necessarily implies the liquefaction of the materials (which may have been caused by earthquakes) and thus the presence of water while the top layer is interpreted as an aeolian deposit.

Nevertheless, the watertable may have played that role while it was barely surfacing. An earthquake may have caused this phenomenon. With its good sorting, its clear granulometric mode and the presence of important shocks on the quartz grains, making them more or less mat, is interpreted as an aeolian deposit formed by the reshuffling of the alluvial grains. This top red ochreous layer was observed in all the stratigraphies.

Thus the stratigraphies of Vabkent, Bash tepe, Tarab and Zaman Baba are formed, at their bottom, by a more or less complex alluvial sequence of average-sized or fine bedded sands topped by massive sand with a generally lighter colour, red ochreous, whose aeolian nature has been demonstrated on the Zaman Baba sediment. The small average size of the grains and the enrichment of the deposit in fine grains made visible by the asymmetry of the granulometric curves indicate that those channel silt deposits at the end of the alluvial course took place downstream. Only the sediment found on the first bifurcation far upstream from Bukhara (North-East) show a very dynamic, coarse nature and are composed of at least two overlying alluvial sequences.

3.4 Dating the paleochannels

Based on correlation between the period, the archaeological surveys and the OSL dating (Tables 1 and 2), we obtain the following data (Fig. 6):

One paleo-channel (OSL7) dates back to the last glacial period (29.2 ka). There is no archaeological settlement around this area.

Two channels were active during the Neolithic (OSL8 and OSL3-4). In the upper part of the oasis, the northern paleo-channel surveyed and dated (sample OSL8) presents in its ending path a series of Neolithic sites which have been well studied by the French-Uzbek Archaeological Mission (MAFANAC-Ajakagytma 2005-2015; since 2015 MAFAC) directed by Frédérique Brunet (Brunet 2005: Fig. 2, 2011: Fig. 2; Brunet et al forthcoming in 2016)[5]. In the western part of the oasis, recent surveys made by the French Archaeological Mission of the Bukhara Oasis (MAFOUB) directed by Rocco Rante identified a few traces of the Kel'teminar culture (through comparisons with the material previously published by Frédérique Brunet (2005, 2011) along the western channel dated through samples OSL 3 - 4.

[5] Frédérique Brunet in 2012 already orally enounced the hypothesis concerning the dynamic of transformation of this northern part of the Zerafshan delta.

Two channels were active from the Late Neolithic to the Bronze Age (OSL 1-2 and OSL 5-6). In the southwestern part of the oasis, previous surveys under the direction of Guljamov et al (1966) brought to light traces of Neolithic and Bronze Age culture along the channel which crosses the so-called "Zaman Baba" area (samples OSL 5-6) and further to the West (Guljamov et al 1966: Figs. 3 and 4). Less clear, but nevertheless identified by the Italian Archaeological Mission directed by Chiara Silvi Antonini (Cerasuolo 2009: Fig. D48), seems to be the identification of Neolithic and Bronze Age traces in the western part of the oasis, along the channel crossing the so-called Bash Tepe area.

Globally we observed a displacement from the river Zerafshan from an active fan centered on the Bukhara oasis to a more active recent one centered on the Qaraqöl oasis.

4 Discussion

Our reconstruction demonstrates the extreme mobility of the Zerafshan river. The dynamics that explains this channel change is due to a classic avulsion process. Globally the direction is guided by neotectonic deformation (active land subsidence (synclinal deformations) and uplift movements (anticlinal deformations) at the scale of the Quaternary.

Nevertheless, if neotectonic forcing creates a potential for a change, an extreme flood event would be needed to change the river course. If we cannot exclude some exceptional floods due to

Table 1. Luminescence dating results

Sample	localization			IR-OSL			BL-OSL		
	Easting (en DMS) WGS84	Northing (en DMS) WGS84	depth (m)	De	a-value	g-value	De	a-value	g-value
Bash Tepe OSL1	63°53'47.882"E	39°54'27.973"N	1.195	10.3 (0.2)	0.025 (0.001)	3.2 (0.1)	16.5 (0.4)	0.036 (0.001)	2.4 (0.1)
Bash Tepe OSL2	63°53'47.882"E	39°54'27.973"N	0.695	8.8 (0.2)	0.024 (0.001)	3.5 (0.2)	11.4 (0.2)	0.026 (0.001)	2.8 (0.4)
Tarab OSL3	63°44'27.18"E	39°44'27.18"N	0.975	15.5 (0.1)	0.028 (0.001)	4.3 (0.2)	18.6 (0.5)	0.024 (0.001)	2.7 (0.3)
Tarab OSL4	63°44'27.18"E	39°44'27.18"N	0.725	15.5 (0.1)	0.034 (0.001)	3.4 (0.3)	18 (0.5)	0.042 (0.001)	1.5 (0.2)
Zaman Baba OSL5	63°51'40.088"E	39°36'49.117"N	1.195	9.3 (0.4)	0.025 (0.001)	5.5 (0.1)	9.6 (0.7)	0.025 (0.003)	3.3 (0.1)
Zaman Baba OSL6	63°51'40.088"E	39°36'49.117"N	0.695	9.1 (0.2)	0.023 (0.001)	4.9 (0.1)	11.2 (0.2)	0.031 (0.001)	2.9 (0.4)
Neo-recent OSL7	63°53'00.893"E	40°13'52.886"N	97.5	49.0 (0.7)	0.028 (0.002)	4.0 (0.1)	53.3 (1.6)	0.035 (0.003)	2.8 (0.4)
Kel' Terminar OSL8	64°51'39.554"E	40°11'50.725"N	45.5	10.3 (0.5)	0.022 (0.002)	4.6 (0.3)	12.7 (0.5)	0.035 (0.002)	3.3 (0.3)

Notes:
depth - mean depth of the layer where was found the sample;
De - beta equivalent dose to the archaeological dose received by the sample since its last solar exposure - unit Gray – Gy;
a-value - alpha efficiency;
g-value - fading rate - correction factor due to anomalous fading - unit percent per decade -% / decade;
The reported uncertainties (values between bracket) correspond to the standard measurement uncertainties (standard deviation).

Table 2. Dosimetry Analysis

Sample	U (ppm)	Th (ppm)	K2O (%)	Dα (mGy/a)	Dβ (mGy/a)	Dγ (mGy/a)	Dcos (mGy/a)	Age (ka)
Laboratory measurements								
Bash Tepe OSL1	1.4(0.1)	4.3(0.4)	1.9(0.3)	1.3	1.4	0.7	0.179	6.66(0.81)
Bash Tepe OSL2	2.1(0.2)	6.8(0.7)	1.9(0.3)	2.0	1.6	0.9	0.191	4.89(0.57)
Tarab OSL3	1.7(0.2)	5.3(0.5)	1.9(0.3)	1.7	1.5	0.8	0.183	9.15(0.87)
Tarab OSL4	1.8(0.2)	5.8(0.6)	1.9(0.3)	1.7	1.5	0.8	0.189	7.89(0.71)
Zaman Baba OSL5	1.8(0.2)	5.7(0.6)	1.9(0.3)	1.7	1.5	0.8	0.179	5.99(0.74)
Zaman Baba OSL6	1.8(0.2)	5.8(0.6)	1.9(0.3)	1.7	1.5	0.8	0.191	5.82(0.70)
Neo-recent OSL7	1.9(0.2)	5.9(0.6)	1.9(0.3)	1.8	1.5	0.8	0.184	29.2(3.4)
Kel' Terminar OSL8	1.8(0.2)	5.6(0.6)	1.9(0.3)	1.7	1.5	0.8	0.197	6.58(0.82)
In-situ gamma spectrometry								
Tarab OSL3	1.80	5.59	1.92			0.872(0.021)		
Tarab OSL4	1.81	5.47	1.91			0.871(0.022)		

Notes:
Laboratory measurements
U, Th - uranium and thorium content based on alpha counting- - Unit ppm;
K2O - potassium oxyde content, arbitrary value following in-situ measurement in Tarab trench - Unit %;
Dα - alpha dose rate Dα = (2.31 U . au + 0.611 Th . ah) / (1+ 1.5 WF) - mGy/a;
Dβ - beta dose rate Dβ = (0.146 U . bu+ 0.0273 Th . bh + 0.649 K2O . bk) / (1+ 1.25 WF) - mGy/a;
Dγ - gamma dose rate Dγ = (0.113 U + 0.0476 Th + 0.202 K2O) / (1+ 1.14 WF) - mGy/a;
(WF – moisture content 5.0 ± 3.0%; au, ah attenuation factors for alpha particles based on Brennan et al 1991; bu, bh, bk attenuation factors for beta particles based on Brennan 2003);
In situ measurements
U, Th, K2O radionuclide contents based on windows count-rate (Aitken 1985);
Dγ - gamma dose rate based on threshold count-rateDcos - cosmic dose rate - as a function of the depth d, based on Prescott and Hutton's (1994) formula $Dcos(d) = Dcos(0)\ exp(-0.15d+0.002d^2)$-mGy/a. Dcos(0) cosmic dose rate at the geomagnetic latitude and altitude of sampling site (Prescott and Hutton 1994, Appendix);
Da - annual dose rate - mGy/a;
Age - Age from the last solar exposure, based on Bayesian numerical stimulation (Zink 2013).

exceptional input on the water drainage in Tadjikistan, from our point of view the hydrological regime of the Zerafshan river cannot account for all the avulsions we were able to map.

4.1 The role of mass-movement in the Zerafshan valley

The transition between the Last Glacial Maximum and the Holocene saw the decline of glaciers. In the upper Zerafshan valley the melting of glaciers triggered mass-movement on slopes, possibly caused by an earthquake, which generated temporary dams. A series of such mass movements has been mapped by Russian geologists (Strom 2013). The breaking of a temporary dam generates a wave which is powerful enough to cause an avulsion 600 km downstream. To validate this hypothesis a systematic mapping of ancient mass movements should be done on the upper Zerafshan and they should be dated. The correlation with the dates of avulsions in Bukhara oasis is the only way to demonstrate our hypothesis.

4.2 The role of Holocene climatic aridification

Central Asia is under the influence of four climatic systems (mid-latitude westerlies, eastern Mediterranean cyclones, Siberian highs and Asian monsoons) which may have impacted temperature and precipitation changes in the past. The orography and the continentality of the region explain the particular aridity of the climate and the type of vegetation made of shrubby and herbaceous steppe ecosystems that dominate the lowlands. The openness of the vegetal landscape may have influenced the hydrological functioning of the fluvial network. Knowledge on climate changes during the Holocene specifically in Uzbekistan is rather poor as no continuous archives have been studied until now. Chen et al (2008) hypothesize that during the Holocene, in Central Asia, the climate was dry at the beginning, wetter or less dry from early to mid-Holocene and moderately wet in the upper part of the Holocene. Rapid climatic events have been identified from many fossil sequences globally distributed on the planet at 9,000-8,000, 6,000-5,000, 4,200-3,800, 3,500-2,500, 1,200-1,000, and 600-150 cal yr BP (Mayewski et al 2004). Most of them correspond to polar cooling and tropical aridity (Mayewski et al 2004). In the Mediterranean basin and in the Middle East, dramatic climatic changes (increase in aridity) were identified at 8,200 cal yr BP (Alley et al 1997, Davis and Stevenson 2007, Pross et al 2009) and around 5,300-5,000, 4,500-3,900, and 3,100-2,800 cal yr BP (Chen et al 2008, Roberts et al 2011). In the Aral Sea basin (Central Asia), during the last two millennia, a cold and arid climate is recorded between 0 and 400 CE, 900 and 1,150 CE, and 1,500 to 1,650 CE; conversely, an increase in moisture is observed between 400 and 900 CE, and 1,150 and 1,450 CE (Sorrel et al 2007). Generally, the majority of authors explain the abandonment of archaeological sites, especially for the Neolithic and the late Bronze Age, by global climate changes and regional and local aridification. The correlation between the abrupt collapse of civilizations and the shift to more arid conditions is clear for some authors (Cullen et al 2000, Kaniewski et al 2013) and less obvious for others (Knapp and Manning 2016).

Our results suggest that in some cases a change in the Zerafshan river course may have been the cause of a drastic change indicating that climatic factors could have been involved. However, human causes cannot be excluded. The discrimination between natural and anthropogenic determinism is not easy to make because of the scarcity of paleoenvironmental knowledge in the Bukhara and Qaraqöl oases and as a whole in Uzbek lowlands.

4.3 Historical consequence of the shifting to southwest of the Zerafshan river after the 4th century BCE

Sites located along the present time Zerafshan main channel, and around Qaraqöl and Paykend, are for the oldest ones from 3rd - 2nd centuries BCE. Before this period the human occupation was mainly concentrated at the end of channels. The inner oasis seems to be largely unoccupied, also probably because of its still marshy ground.

We can hypothesize that the Qaraqöl alluvial fan has been active since the 4th century BCE. It means that before the 4th century BCE the Zerafshan together with the Kaska Daria rivers were parallel to the Amu Daria and that the marshy lands in their flood plain were an obstacle for human presence. It would be interesting to consider the hypothesis that the Silk Road was only possible in this area after the 4th century BCE.

5 Conclusion

Our regional study emphasised the importance of channel migration of the river Zerafshan at the surface of the alluvial plains of Bukhara and Qaraqöl which results from the coalescence of a succession of paleo-channels, at least 8 for the Zerafshan river itself.

From the Neolithic to the Bronze Age settlements are strictly dependent on the vicinity of an active channel to irrigate the land. After this period, the development of a complex irrigation system implies a complex channel network linking them and sophisticated management of the hydraulic flow.

Our main results are to emphasise that avulsions may have been caused by mass movement in the upper Zerafshan at the origin of the collapse of temporary dams generating catastrophic floods and that the cause of abandonment of human settlements can be found in a change of the river course and is not systematically due to a climatic arid crisis.

Our program will continue to proceed with OSL sampling for the last three paleo-channels identified for the Zerafshan river and we will extend our survey in the Qaraqöl Oasis.

Acknowledgements

We would like to thank Cecile Fouache, Senior Lecturer at the University of Rouen, for the English reading and translation of this article and Florence Bonnaud, cartographer at the University of Paris Sorbonne.

References

Abdullaev, I., 2004. The analysis of water management in Bukhara oasis of Uzbekistan: historical and territorial trends. Water International, **29**(1): 20 - 26.

Adylov, Š.T., 2002. Zapadnye okrainy bucharskogo oazisa na rannich stadijach obživanija (VI v. do n.e. – III v. n.e.). Istorija material’noj kul’tury Uzbekistana, **33**: 72 - 80.

Aitken, M.J., 1985. Thermoluminescence Dating. Academic Press, Orlando, Florida

Alley, R.B., P.A. Mayewski, T. Sowers, M. Stuiver, K.C. Taylor and P.U. Clark, 1997. Holocene climatic instability: a prominent, widespread event 8200 yr ago. Geology, **25**: 483 - 486.

Askarov, A.A., 1965. Novye nachodki andronovskoj kul´tury v nizov´jach Zarafšana. Istorija material´noj kul´tury Uzbekistana, **6**: 53 - 60.

Askarov, A.A., 1981. K peredatirovke kul´tury Zamanbaba. In: Itina, M.A.. (ed.), Kul´tura I iskusstvo drevnego Chorezma. Rapoport. Moscow, Nauka, 99 - 110.

Bossu, R., 1996. Etude de la sismicité intraplaque de la région de Gazli (Ouzbekistan) et localisation de la déformation sismique. Thèse de l’Université Joseph Fourier-Grenoble.

Brennan, B.J., 2003. Beta doses to spherical grains. Radiation Measurements, **37**: 299 - 3003.

Brennan, B.J., R.G. Lyons and S.W. Phillips, 1991. Attenuation of alpha particle track dose for spherical grains. Nuclear Tracks and Radiation Measurements, **18**: 249 - 253.

Brunet, F., 2005. Pour une nouvelle étude de la culture néolithique de Kel’terminar Ouzbekistan. Paléorient, **31**(2): 87 - 105.

Brunet, F., 2011. Comment penser la néolithisation en Asie Centrale (Xe-IVe millénaires)? L’émergence de nouveaux modèles de sociétés entre sédentaires et nomades. Paléorient, **37**(1): 187 - 204.

Brunet, F., Khudzhanazarov M. and Hoshimov H. (eds.), La néolithisation en Ouzbékistan: étude de la culture de Kel'teminar (VII^{e}-V^{e} millénaires av. n. è.). Le site d’Ajakagytma et la région du Bas-Zeravshan. De Boccard, collection MAFACAM n°18 : Paris (forthcoming).

Burjakov, Ju.F. and G.A. Košelenko, 1985. Taškentskij oazis (Čač). In: Košelenko, G.A. (ed.), Drevnejšie gosudarstva Kavkaza i Srednej Azii. Moscow, Nauka, 297 - 303, pls. CXLVIII, CXLIX, 46 - 48.

Cerasuolo, O., 2009. Indagine topografica nel territorio di Varakhsha. In: Antonini, C.H. and D. Mirzaakhmedov (eds.), Gli scavi di Uch Kulakh (oasis di Bukhara), 189 - 216.

Chen, F., Z. Yu, M. Yang, E. Ito, S. Wang, D.B. Madsen, X. Huang, Y. Zhao, T. Sato, H.J.B. Birks, I. Boomer, J. Chen, C. An and B. Wünnemann, 2008. Holocene moisture evolution in arid central Asia and its out-of-phase relationship with Asian monsoon history. Quaternary Science Reviews, **27**: 351 - 364.

Cullen, H.M., P.B. de Menocal, S. Hemming, G. Hemming, F.H. Brown, T. Guiderson and F. Sirocko, 2000. Climate change and the collapse of the Akkadian empire: Evidence from the deep sea. Geology, **28**(4): 379 - 382.

Davis, B.A.S. and A.C. Stevenson, 2007. The 8.2 ka event and early-mid Holocene forests, fires and flooding in the Central Ebro Desert, NE Spain. Quaternary Science Reviews, **26**: 1695 - 1712.

Fouache, E., R. Besenval, C. Cosandey, C. Coussot, M. Ghilardi, S. Huot and M. Lamothe, 2012. Palaeo-Channels of the Balkh River (Northern Afghanistan) and human occupation since the Bronze Age period. Journal of Archaeological Science, **39**: 3415 - 3427.

Gardin, J.C. and P. Gentelle, 1979. L'exploitation du sol en Bactriane antique. Bulletin de l'Ecole Francaise d'Extrême Orient 66.

Guljamov, Ja.G., U.I. Islamov and A.A. Askarov, 1966. Pervobithaja kultura I vozniknovenie oroshaemogo zemledelija v nizovjakh Zarafshana, Tashkent.

Kaniewski, D., E. van Campo, J. Guiot, S. Le Burel, O.T. Thierry and C. Baeteman, 2013. Environmental roots of the Late Bronze Age crisis. Plos One, **8**: 1 - 10.

Knapp, A.B. and S.W. Manning, 2016. Crisis in context: the end of the late Bronze Age in the Eastern Mediterranean. American Journal of Archaeology, **120**(1): 99 - 149.

Litvinskij, B.A., 1972. Drevnie kochevniki "Kryshi mira", Moscow.

Litvinskij, B.A., 1976. Das K'ang-chu-Sarmatische Farn. Central Asian Journal, **20**: 47 - 74.

Lo Muzio, C., 2009. An archaeological outline of the Bukhara oasis. Journal of Inner Asian Art and Archaeology, **4**: 43 - 68.

Mayewski, P.A., E. Eelco, E.E. Rohling, J.C. Stager, W. Wibjfrn Karle´n, A Kirk, K.A. Maasch, L.D. Meeker, E.A. Meyerson, F. Gasse, S. van Kreveld, K. Holmgren, J. Lee-Thorp, G. Rosqvist, F. Rack, M. Staubwasser, R.R. Schneider and E.J. Steig, 2004. Holocene climate variability. Quaternary Research, **62**: 243 - 255.

Olsson, O., M. Gassmann, N. Manig, M. Ikramova and K. Wegerich, 2013. Basin efficiency approach and its effect on streamflow quality, Zerafshan River Uzbekistan. Journal of Hydrology, **476**: 128 - 135.

Prescott, J.R. and J.T. Hutton, 1994. Cosmic ray contributions to dose rates for luminescence and ESR dating: large depths and long-term time variations. Radiation Measurements, **23**: 497 - 500.

Pross, J., U. Kotthoff, U.C. Müller, O. Peyron, I. Dormoy, G. Schmiedl, S. Kalaitzidis and A.M. Smith, 2009. Massive perturbation in terrestrial ecosystems of the Eastern Mediterranean region associated with the 8.2 ka climatic event. Geology, **37**: 887 - 890.

Rante. R., 2013. Les fouilles de Paykend: nouveaux éléments, dans 25 ans d'archéologie française en Asie Centrale. Nouvelles méthodes, nouvelles perspectives, Julio Bendezu-Sarmiento éd., de Boccard, Paris.

Roberts, A.P., E.J. Rohling, K.M. Grant, J.C. Larrasoana and Q. Liu, 2011. Atmospheric dust variability from Arabia and China over the last 500,000 years. Quaternary Science Reviews, **30**: 3537 - 3541.

Šiškin, V. A., 1963. Varachša. Akademija Nauk SSSR, Moscow, 17.

Šiškin, V. A., 1955. Raskopki v meč.eti Magaki-attari v Buchare. Trudy Instituta istorii i archeologii Akademija Nauki UzCCR, **7**: 29 - 60.

Sorrel, P., S.P. Popescu, S. Klotz, J.P. Suc and H. Oberhänsli, 2007. Climate variability in the Aral Sea basin (Central Asia) during the late-Holocene based on vegetation changes. Quaternary Research, **67**: 357 - 370.

Strom, A., 2013. Geological prerequisites for landslide dam's disaster assessment and mitigation in central Asia. In Wang, F. et al. (eds), Progress of Geo-Disaster Mitigation Technology in Asia, Environmental Science and Engineering. Springer Verlag, 17 - 52

Zimmerman, D.W., 1971. Thermoluminescent dating using fine grains from pottery. Archeometry, **13**: 29 - 52

Zink, A., 2008. Uncertainties on the Luminescence Ages and anomalous fading. Geochronometria, **32**: 47 - 50.

Zink, A.J.C., 2013. A coarse Bayesian approach to evaluate luminescence ages. Geochronometria, **40**: 90 - 100.